ES Energy & Environment

RESEARCH PAPER View Article Online

Tunable Formation of ZnSe to ZnO due to a Controlled Phase Transition Driven by Hydrazine and Sodium Hydroxide

Fen Qiao[1*], Qichao Liang[1], Xuejun Cui[2], Qian Xu[3], Yi Xie[4] and Huaqiang Chu[5*]

Controllable ZnSe and ZnO structures with different morphologies were synthesized by a simple hydrothermal method. The effects of hydrazine hydrate and sodium hydroxide on the final product and morphology were studied. The results showed that controlled phase transition from ZnSe to ZnO was achieved by adjusting the volume of hydrazine hydrate. The structure variety of as-synthesized product depended on the hydrazine hydrate volume and sodium hydroxide concentration, which was further confirmed by SEM and XRD. It showed that hydrazine hydrate acted a pivotal part in the restoring process of selenium. Pure ZnSe microspheres were obtained when the volume of $N_2H_4 \cdot H_2O$ increased to 10 mL. While the final product completely changed into ZnO rods when the $N_2H_4 \cdot H_2O$ was absent during the synthesize process. Additionally, when the concentration of NaOH was higher than 0.5 M, ZnO tended to self-assemble into flower-like ZnO structures. The corresponding reaction mechanism was discussed. The current-voltage characteristics indicated that self-assembled flower-like ZnO structures displayed excellent electrical properties, which was attributed to the special structural feature with large specific surface area and defect states formed by adjusting the sodium hydroxide concentration. This facile approach for phase transition from ZnSe to ZnO may provide an alternative way for preparation of functional heterostructure, which demonstrates their potential application in optoelectronic devices.

Keywords: ZnSe; ZnO; Morphology; Phase Transition

Received 1 October 2018**, Accepted** 3 December 2018

DOI: 10.30919/esee8c187

1. Introduction

ZnSe and ZnO have emerged interest as potential candidates for electronic materials owing to their high conductivity and electron mobility,[1-5] resulting in broad applications in high-temperature,[6] high-frequency,[7,8] anti-radiation,[9] short-wavelength luminescence areas.[10] It is well known that the properties of those devices depend on morphology and structure, which in turn affects the carrier transport performance of materials. Many efforts have been devoted to synthesizing ZnO and ZnSe with various morphologies, such as chemical vapor deposition method,[11,12] spray deposition,[13] thermal evaporation,[14] vapor-liquid-solid method[15] and pulse laser deposition technology.[16,17] However, these methods are typically time consuming and the experimental conditions are rigorous, which severely restrict their practical applications in electronic devices. So, it is highly desirable to develop a facile and effective synthesis approach. In addition, although various ZnO or ZnSe structures with different morphologies have been reported, no further studies have been reported on the tunable phase transitions from ZnSe microspheres to rod-like ZnO structures and their electronic properties.

Here, a facile hydrothermal method for the synthesis of ZnSe microspheres and ZnO rods was demonstrated. The ZnSe microspheres suffered obvious morphological and phase change into ZnO rods when the $N_2H_4 \cdot H_2O$ was absent. And the length of ZnO rods was further decreased when the $N_2H_4 \cdot H_2O$ and Na_2SeO_3 were absent. Interestingly, the ZnO rods tended to self-assembly into flower-like ZnO structures with appropriate concentration of NaOH. The correlative electrical properties of ZnSe microspheres and ZnO rods were also investigated, and it was found that the self-assembled ZnO flowers exhibited the best electrical performance. The difference in electrical performance was due to the different specific surface area and defect states generated with various concentration of sodium hydroxide.

2. Experimental

2.1 Preparation of ZnSe microspheres and ZnO rods

All chemicals used without further purification were of analytical grade, which were purchased from Sinopharm Chemical Reagent Co., Ltd (China). ZnSe microspheres and ZnO rods were synthesized by hydrothermal method. Typically, 30 mL of $Zn(NO_3)_2 \cdot 6H_2O$ (0.03 M), Na_2SeO_3 (0.03 M) and NaOH (0.67 M) were prepared by stirring at room temperature for 20 min. Then, 10 mL $N_2H_4 \cdot H_2O$ (85%, v/v) solution was added into the above solution under vigorous stirring. Subsequently, the mixture was put into a Teflon-sealed autoclave and kept at 180 °C for 4 h, and then cooled to room temperature. The resulting products were collected by centrifugation (1500 rpm, 5 min) and then washed twice with ethanol. Finally, the products were annealed at 60 °C in the air for further characterization. In addition, the effects of $N_2H_4 \cdot H_2O$ volume and NaOH concentration on the structure

[1]*School of Energy and Power Engineering, Jiangsu University, Zhenjiang, 212031, China*
[2]*College of Chemistry, Jilin University, Changchun 130012, China*
[3]*Institute for Energy Research of Jiangsu University, Jiangsu University, Zhenjiang 212031, China*
[4]*State Key Laboratory of Silicate Materials for Architectures, Wuhan University of Technology, Wuhan 430070, China*
[5]*School of Energy and Environment, Anhui University of Technology, Ma'anshan 243002, China*
***E-mail:** fqiao@ujs.edu.cn; hqchust@163.com*

and morphology of the products were also investigated.

2.2 Characterization

Structure and morphology of samples were characterized by X-ray diffraction (XRD, Philips 1730) and Field Emission Scanning Electron Microscopy (FESEM, JSM-7800F), respectively. The absorption spectra were investigated in the range of 200-800 nm by UV-Vis absorption spectroscopy (UV-3600 Plus). Current-voltage characteristics (*I-V*) were carried out at room temperature using a Keithley 2400 source meter.

3. Results and discussion

3.1 Morphology and Structure Characteristics

Fig. 1a-b present the SEM images of the products synthesized with $N_2H_4{\cdot}H_2O$ in different volumes. A large amount of ZnO rods and raw ZnSe microspheres were obtained with 0.2 mL of $N_2H_4{\cdot}H_2O$ (Fig. 1). When the volume of $N_2H_4{\cdot}H_2O$ was 5 ml, a large amount of ZnSe microspheres and some ZnO rods were discovered (Fig. 2a). As the volume of $N_2H_4{\cdot}H_2O$ increased to 10 ml, only ZnSe microspheres were achieved (Fig. 2b). Some ZnSe microspheres with diameters of ~5 μm were observed. The SEM observations indicated that the volume of $N_2H_4{\cdot}H_2O$ had a significant effect on the structure change from ZnO to ZnSe.

The corresponding XRD pattern is shown in Fig. 2c. When the volume of $N_2H_4{\cdot}H_2O$ was 5 ml, the diffraction peaks of the microsphere

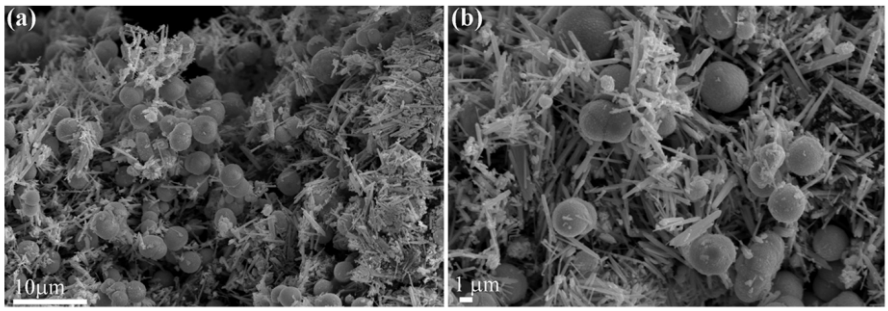

Fig. 1 Low- and High- magnification SEM images of final products prepared with 0.2 mL $N_2H_4{\cdot}H_2O$ and 0.67 M NaOH.

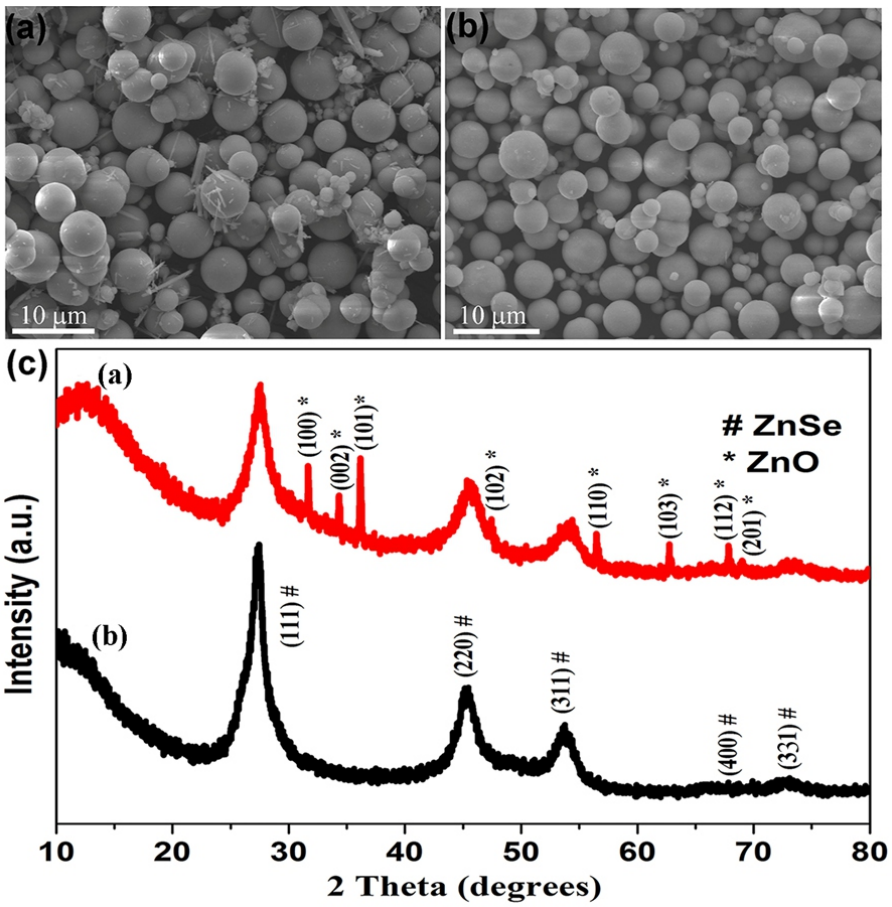

Fig. 2 FESEM images and XRD patters of final products prepared with 0.67 M NaOH and different volume of $N_2H_4{\cdot}H_2O$: (a) 5 ml, and (b)10 ml.

(Fig. 2a) could be well indexed to cubic ZnSe (JCPDS#37-1463).

Besides, the relatively weak peaks marked with asterisk were from hexagonal wurtzite ZnO (JCPDS#36-1451). While the obtained diffraction peaks originated from the cubic ZnSe (JCPDS#37-1463) when the volume of $N_2H_4 \cdot H_2O$ reached to 10 mL. In addition, the diffraction peaks of ZnSe sample became narrower and no other impurity peaks were observed (red curve), compared with another sample (Fig. 2a), which indicated that the growth of ZnSe crystals had high purity.

To further investigate the influence of NaOH on morphology and structure, the $N_2H_4 \cdot H_2O$ was absent and the concentration of Na_2SeO_3 was kept at 0.03 M. Fig. 3a-d present SEM images of the ZnO samples, which were prepared with different concentration of NaOH. As shown in Fig. 3a, rod-like ZnO structure with diameter ~0.5 μm and length ~4.5 μm was obtained when the concentration of NaOH was 0.4 M. And the ZnO rods began to self-assemble into clusters at 0.5 M NaOH (Fig. 3b). A large quantity of flower-like microstructures were self-assembled when the concentration of NaOH arrived at 0.67 M, and each flower was made up of multiple ZnO rods, which grew radially from the center (Fig. 3c). When the concentration of NaOH climbed to 1 M, ZnO rods with longer length were observed (Fig. 3d). Fig. 3e exhibits the XRD patterns of four as-synthesized samples, all diffraction peaks of four samples could be precisely assigned to the hexagonal wurtzite ZnO (JCPDS #36-1451), which also confirmed the high purity of ZnO and the absence of other detectable phases in the XRD pattern.

According to the above results, we proposed that the Na_2SeO_3 precursor may have no effect on the final product and its structure when $N_2H_4 \cdot H_2O$ was absent. Under the condition of keeping other parameters

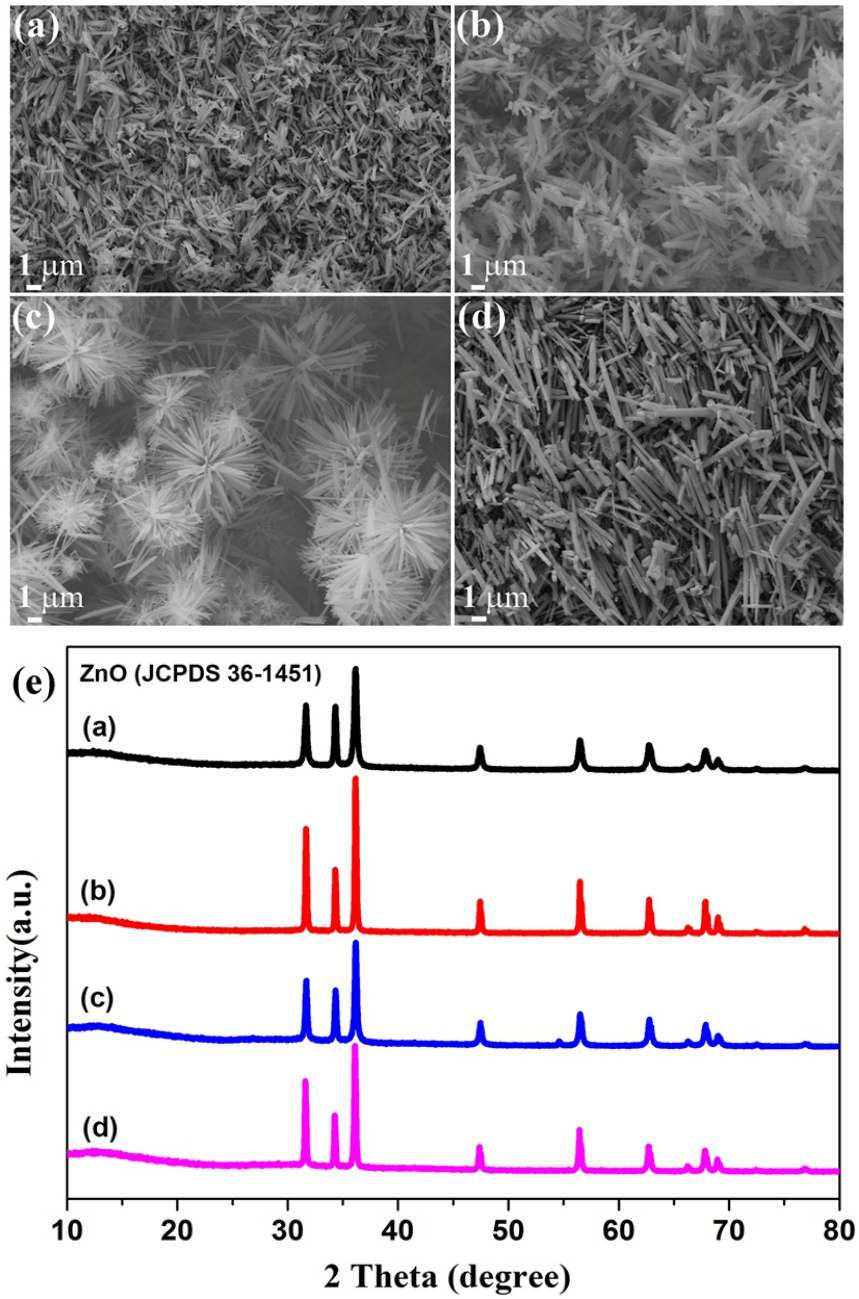

Fig. 3 FESEM images and XRD patterns of final products synthesized with various concentrations of NaOH (a-d): 0.4 M, 0.5 M, 0.67 M, and 1 M, in which $N_2H_4 \cdot H_2O$ was absent and the concentration of Na_2SeO_3 was 0.03 M.

constant, experiments without $N_2H_4 \cdot H_2O$ and Na_2SeO_3 were carried out. SEM images of ZnO prepared without $N_2H_4 \cdot H_2O$ and Na_2SeO_3 are shown in Fig. 4a-d. The morphology of ZnO rods was similar to that of ZnO prepared in the absence of $N_2H_4 \cdot H_2O$ (Fig. 3). The clear difference was that the length of ZnO rods and the self-assembled flower-like ZnO rods became much more shorter, compared with the samples of Fig. 3b-c. As the concentration of NaOH exceeded 0.5 M, the ZnO rods also self-assembled into flower-like structure, in which the ZnO rods were scattered from center.

Fig. 4e demonstrated that all XRD peaks of four products corresponded to ZnO with hexagonal wurtzite structure (JCPDS#36-1451). The room temperature UV-Vis absorbance spectra of the pure ZnSe microsphere and ZnO samples were shown in Fig. 5. It was observed that ZnSe displayed absorption peak at around 460 nm, and the bandgap of the ZnO sample calculated from their central peak position was approximately 3.3 eV, which was close to the theoretical value.[18]

To explain the main origin of the interaction among Zn^{2+}, Se^{2-} and $N_2H_4 \cdot H_2O$ during the synthesis transformation process (Fig. 6), it would be of great meaningful to describe the formation of ZnSe microspheres, as shown in the following equations (1)-(2):

$$2\,N_2H_4 \bullet H_2O + 2\,OH^- + SeO_3^{2-} \rightarrow 2\,N_2 + Se^{2-} + 7\,H_2O \quad (1)$$

$$Se^{2-} + Zn^{2+} \rightarrow ZnSe \quad (2)$$

In this work, $N_2H_4 \cdot H_2O$ and Na_2SeO_3 were chosen as reducing agent and Se source, respectively, and NaOH provided a good alkaline

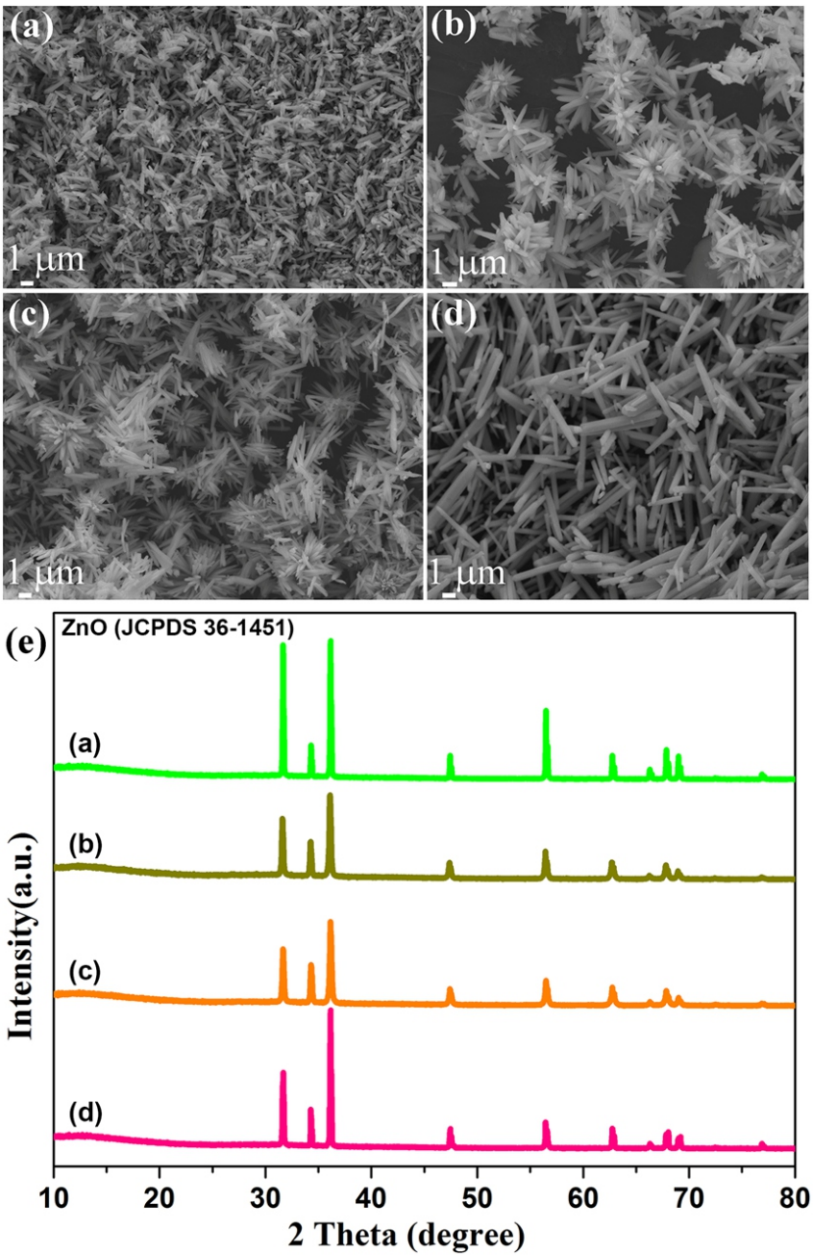

Fig. 4 SEM images and XRD patters of final products synthesized with various concentrations of NaOH (a-d): 0.4 M, 0.5 M,0.67 M, and 1M, in which $N_2H_4 \cdot H_2O$ and Na_2SeO_3 were absent.

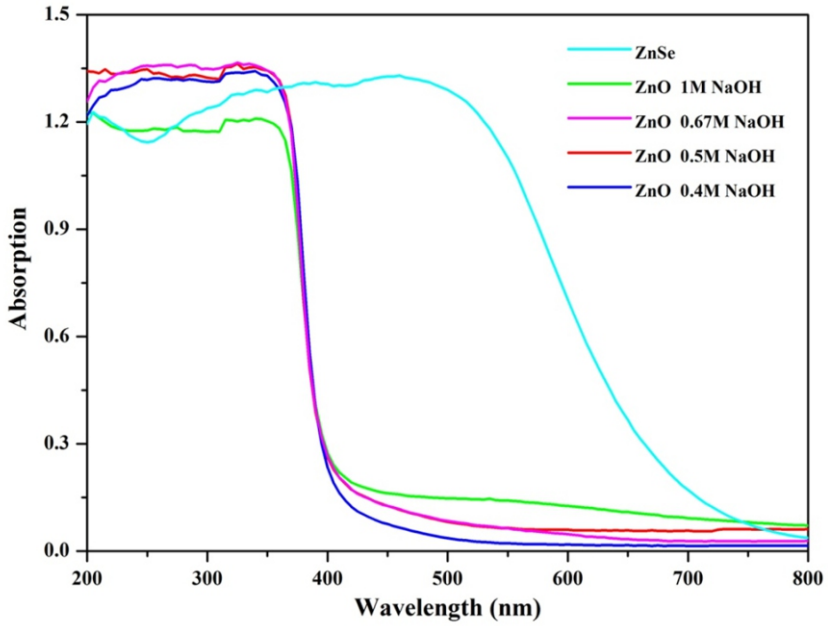

Fig. 5 UV-Vis absorption spectra of pure ZnSe microspheres (a) pure ZnO rods obtained with different concentration of NaOH (b) 1 M, (c) 0.67 M, (d) 0.5 M, (e) 0.4 M, in which Na_2SeO_3 was absent.

environment. $N_2H_4{\cdot}H_2O$ worked as a reducing agent and reduced the SeO^{2-} to Se^{2-} ions at 180 ˚C according to the reaction equation (1), these Se^{2-} ions reacted with Zn^{2+} and ZnSe microspheres were formed as reaction products. The pure ZnSe microspheres could be obtained when the $N_2H_4{\cdot}H_2O$ was 10 mL. However, when the volume of $N_2H_4{\cdot}H_2O$ decreased from 10 to 5 mL, ZnO phase were also appeared. This may be because the content of $N_2H_4{\cdot}H_2O$ was not enough to reduce all Se, resulting in the residual Zn^{2+} ions in the solution, which would react with OH^-, and then the formed $Zn(OH)_2$ was decomposed into ZnO. Pure ZnO rods were formed when the volume of $N_2H_4{\cdot}H_2O$ was further reduced to 0 ml, which indicated that the $N_2H_4{\cdot}H_2O$ acted a key role in the structure formation of ZnSe. It was also found that the higher NaOH concentration resulted in significantly extended ZnO rods length, which was attributed to the ratio between OH^- ions and Zn^{2+}.[19,20] With the concentration of OH^- increased, a large number of self-assembled ZnO rods with flower-like structure were achieved. It was found that the rods grew in a centrally radiated network structure, which was contributed to surface energy and free Gibbs energy.[21]

Additionally, compared with the ZnO synthesized without Na_2SeO_3, ZnO prepared by Na_2SeO_3 had a minor increase in diameter, indicating that the presence of Na_2SeO_3 had a slight effect on the final diameters of ZnO rods. When the concentration of NaOH was higher than 0.5 M, the tips of ZnO rods synthesized were tapered, which was attributed to the fact that some groups with negative charge tended to

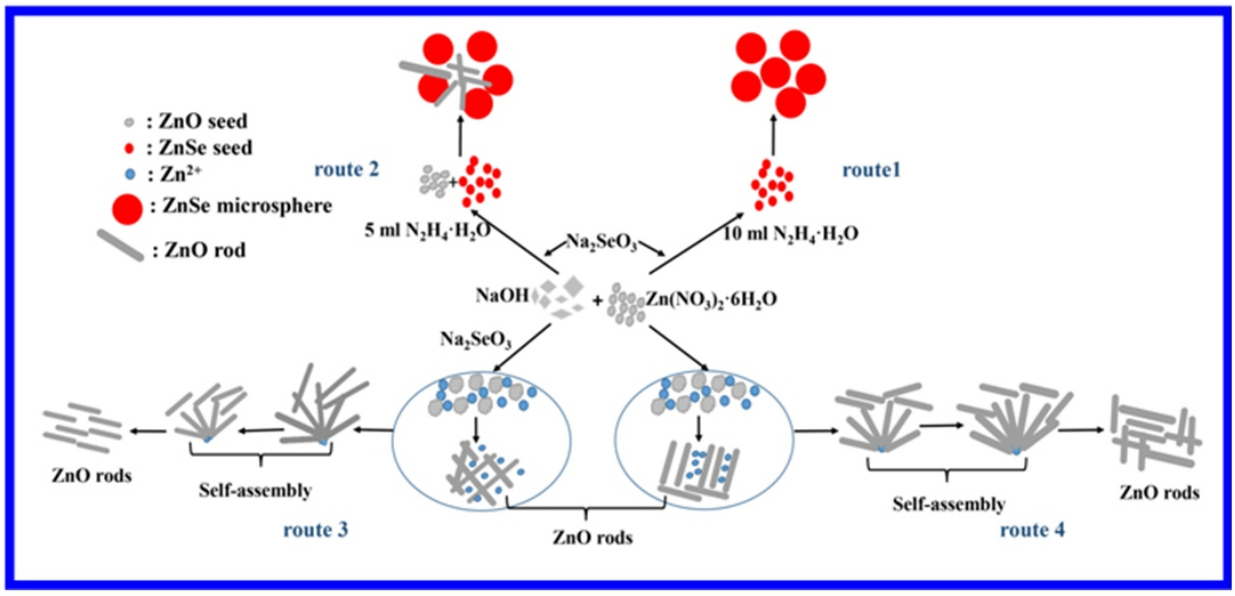

Fig. 6 Schematic illustration of the synthesis of ZnSe microspheres and ZnO rods.

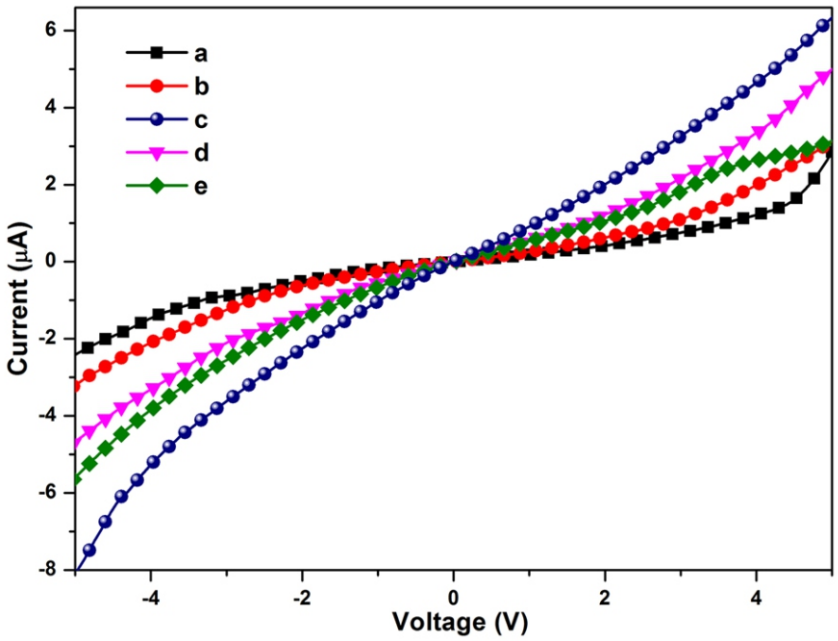

Fig. 7 I-V characteristic curve of (a) ZnSe microspheres, (b-e) ZnO rods obtained with different NaOH concentration (b-e): 1 M, 0.67 M, 0.5 M and 0.4 M.

grow on the positive side of the ZnO crystals.[22,23]

3.2 Electrical characterization

Fig. 5 illustrates the room temperature current-voltage (*I-V*) characteristics of ZnSe microspheres and ZnO rods synthesized with different concentration of NaOH. The results showed that the *I-V* features of all samples appeared to be symmetric with respect to the bias voltage. Additionally, the current of ZnSe microspheres was obviously lower than that of ZnO samples, which could be caused by the presence of oxygen deficiencies or Zn interstitials in the ZnO lattice.[24,25] And the large difference in the conductivity of ZnO prepared with various concentrations of NaOH might be due to the different amount of Zn interstitial. Moreover, the self-assembled ZnO flowers exhibited the highest current compared with other samples, it could be attributed to its larger specific surface area and defect states, which were beneficial to the free electrons transport.

4. Conclusions

Tunable phase transition from ZnSe microspheres into ZnO rods was achieved by adjusting the volume of hydrazine hydrate and the concentration of sodium hydroxide. Pure ZnSe microspheres were formed when the volume of $N_2H_4{\cdot}H_2O$ increased to 10 mL, while large amount of pure ZnO rods were formed when the $N_2H_4{\cdot}H_2O$ was absent. Depending on the different concentration of NaOH, ZnO rods tended to self-assemble into flower-like ZnO structures when the concentration of NaOH was higher than 0.5 M. The related current-voltage characteristics of ZnO flowers displayed the superior electrical properties, which indicated the suitable concentration of sodium hydroxide could significantly affect the formation of defect states in microstructures films and then altered its electronic properties. This facial phase transition method may be exploited for the fabrication of ZnO/ZnSe heterostructures for broad electronic devices applications.

Conflict of Interest

The authors declare no conflict of interest.

Data Availability

The related supplementary data is in the part of supporting information.

Acknowledgements

The authors appreciate the financial support of the National Natural Science Foundation of China (No.51406069), China Postdoctoral Science Foundation Special Project (No.2016T90426), China Postdoctoral Science Foundation (No.2015M581733), Jiangsu Planned Projects for Postdoctoral Research Funds (No.1501107B) and Training Project of Jiangsu University Youth Backbone Teacher.

Reference

1. T. K. Maji, D. Bagchi, P. Kar, D. Karmakar and S. K. Pal, *J. photoch. photobio. A.,* 2017, **332**, 391-398.
2. A. Sahu, R. Chaurashiya, K. Hiremath and A. Dixit, *Sol. Energy,* 2018, **163**, 338-346.
3. X. Zhang, Z. Tang, D. Hu , D. Meng and S. Jia, *Mater. Lett.,* 2016, **168**, 121-124.
4. M. F. Al-Ajmi, A. Hussain and F. Ahmed, *Ceram. Int.,* 2016, **42**, 4462-4469.
5. L. S. R. Rocha, C. R. Foschini, C. C. Silva, E. Longo and A. Z. Simões, *Ceram. Int.,* 2016, **42**, 4539-4545.
6. L. Kong, X. Yin, M. Han, L. Zhang and L. Cheng, *Ceram. Int.,* 2015, **41**, 4906-4915.
7. M. A. Mezdrogina, A. Ya. Vinogradov, V. Levitskii, E. Terukova, Y. V. Kozhanova and A. Aleksandr, *Semiconductors,* 2017, **51**, 559-564.
8. Q. Liu, J. Zhu, N. Ma, T. Wang, L. Wang and H. Yang, *J. Mater. Sci-Mater. El.,* 2017, **28**, 1-9.
9. T. I. Goglidze, I. V. Dementiev, A. V. Coval, E. P. Goncearenco, N. D. Nedeoglo and D. D. Nedeoglo, *J. Lumin.,* 2018, **197**, 396-398.
10. N. Liu, H. Xue, Y. Ji and J. Wang, *J. Alloys Compd.,* 2018, **747**, 696-702.
11. Y. Zhao, C. Li, M. Chen, X. Yu, Y. Chang, A. Chen, H. Zhu and Z. Tang, *Phys. Lett. A.,* 2016, **380**, 3993-3997.
12. G. Escalante, H. Juárez and P. Fernández, *Adv. Powder. Technol.,* 2016, **28**, 23-29.

13. V.Mata, A. Maldonado and M de la Luz Olvera, *Mat. Sci. Semicon. Proc., 2018,* **75**, 288-295.
14. T. Saha, A. A. Mohanan, V. Swamy, N. Guo and N. Ramakrishnan *Mater. Res. Bull.,* 2016,**77**, 288-295.
15. N. H. Alvi, W. U. Hassan, B. Farooq, O. Nur and M. Willander, *Mater. Lett.,* 2013, **106**, 158-163.
16. A. Krämer, S. Engel, N. Sangiorgi, A. Sanson, J. F. Bartolomé, S. Gräf and F. A. Müller, *Appl. Surf. Sci.,* 2017, **399**, 282-287.
17. H. Kumarakuru, D. Cherns and A. M. Collins, *Ceram. Int.,* 2014, **40**, 8389-8395.
18. A. Khorsand Zak, W. H. A. Majid, H. Z. Wang, R. Yousefi, A. Moradi Golsheikh and Z. F. Ren, *Ultrason. Sonochem*., 2013, **20**, 395-400.
19. R. Shi, P. Yang, X. Dong, Q. Ma and A. Zhang, *Appl. Surf. Sci.,* 2013, **264**, 162-70.
20. H. Usui, *J. Colloid. Interf. Sci.,* 2009, **336**, 667-674.
21. A. Lüttge, *J. Electron. Spectrosc.,* 2006, **150**, 248-259.
22. B. Wang, W. Zhong, C. Ye, E. Shi and Z. Yin , *J. Cryst. Growth,* 1996, **160,** 375-381.
23. E. P. Warekois, M. C. Lavine, A. N. Mariano and H. C. Gatos, *J. Appl. Phys.,* 1966, **37**, 2203-2203.
24. Y. Zhang, B. Lin, Z. Fu, C. Liu and W. Han, *Opt. Mater.,* 2006, **28**, 1192-1196.
25. A. Purohit, S. Chander, A. Sharma, S. P. Nehra and M. S. Dhaka, *Opt. Mater.,* 2015, **49**, 51-58.

